

Article

Hybrid Renewable Hydrogen Energy Solution for Application in Remote Mines

Hosein Kalantari ¹, Seyed Ali Ghoreishi-Madiseh ^{1,*} and Agus P. Sasmito ²

¹ NBK Institute of Mining Engineering, University of British Columbia, Vancouver, BC V6T 1Z4, Canada; hoseink@mail.ubc.ca

² Department of Mining and Materials Engineering, McGill University, Montreal, QC H3A 0E8, Canada; agus.sasmito@mcgill.ca

* Correspondence: ali.madiseh@ubc.ca

Received: 9 November 2020; Accepted: 28 November 2020; Published: 2 December 2020



Abstract: Mining operations in remote locations rely heavily on diesel fuel for the electricity, haulage and heating demands. Such significant diesel dependency imposes large carbon footprints to these mines. Consequently, mining companies are looking for better energy strategies to lower their carbon footprints. Renewable energies can relieve this over-reliance on fossil fuels. Yet, in spite of their many advantages, renewable systems deployment on a large scale has been very limited, mainly due to the high battery storage system. Using hydrogen for energy storage purposes due to its relatively cheaper technology can facilitate the application of renewable energies in the mining industry. Such cost-prohibitive issues prevent achieving 100% penetration rate of renewables in mining applications. This paper offers a novel integrated renewable–multi-storage (wind turbine/battery/fuel cell/thermal storage) solution with six different configurations to secure 100% off-grid mining power supply as a stand-alone system. A detailed comparison between the proposed configurations is presented with recommendations for implementation. A parametric study is also performed, identifying the effect of different parameters (i.e., wind speed, battery market price, and fuel cell market price) on economics of the system. The result of the present study reveals that standalone renewable energy deployment in mine settings is technically and economically feasible with the current market prices, depending on the average wind speed at the mine location.

Keywords: renewable energy; hydrogen; wind power; battery storage; thermal storage; remote mining

1. Introduction

Underground mining is among the most energy-intensive industrial activities [1,2]. This is especially true in Canada. In fact, Natural Resources Canada [3] reports that the mining industry consumed a substantial portion of Canada's total industrial secondary energy use in 2017 (1318.5 petajoules). Although some efforts have been made over the last few decades to shift towards green energies, most Canadian mines still consume considerable amount of fossil fuels. Due to this high fossil fuel dependency, the mining sector is the primary contributor of carbon emission from Canadian industry (82.6 megatons in 2017, according to Natural Resources Canada [3]). This energy-environmental problem escalates in remote operations, where there is no electrical grid access or natural gas pipelines, which makes them solely reliant on diesel for provision of power, haulage, and heat [4]. To improve the energy profile of the mining industry, it is evident that far-reaching improvements are necessary.

Renewable energy systems, such as wind and solar photovoltaic (PV), are the most commonly sought alternatives to fossil fuels [5–8], with a few successful cases of implementation in the mining industry. Although both of these systems have worldwide growing interest, based on

Energy Resources data [9], the wind power generation system is economically a more feasible option for Canadian mines. For example, Diavik Diamond Mine, located in the Northwest Territories of Canada, uses four 2.3 MW wind turbines to supply 10% of its electric power. It has been reported that this investment resulted in a \$31 million dollar capital cost. Despite its relatively high upfront cost, the wind power generation system was reported to save \$5 million dollars (3.8 million liters of fuel) in 2013. The payback period of the project is estimated to be eight years [10]. Inspired by the success of the Diavik Diamond Mine, in 2015, Raglan Mine, in Quebec, Canada, installed a 3 MW wind turbine generator coupled with a multi-storage system with a combination of 200 kW/1.5 kWh flywheel, 200 kW/250 kWh Li-ion battery, and 200 kW/1 MWh hydrogenic system. According to Natural Resources Canada [11], the system was able to save 3.4 million liters of diesel and 9110 tons of carbon emission over the first 18 months of its implementation. The second wind turbine was assembled into the renewable system in 2018 [12]. The upgraded system is predicted to replace more than 4.4 million liters of diesel fuel, reduce carbon emission by 12,000 tons, and remove the equivalent of 2700 vehicles off the roads [12].

Although several cases of successful implementations have been reported in mining literature, clean energy systems have not been able to provide the power for off-grid mining. High cost and short lifetime of battery storage systems are among the main restrictive factors to achieve 100% penetration rate of renewables [13,14]. Usually, battery storage represents a sizable portion of a standalone system's overall cost, and it needs to be replaced throughout the mine's lifetime [15]. Alternatively, hydrogen storage systems can help mitigate this issue and facilitate the application of a standalone renewable energy system [16]. Such a storage system includes an electrolyzer, a hydrogen tank, and a fuel cell. The generated power from renewable energy sources (wind turbine or solar system) supplies the power demand, and the surplus energy will be transported to the electrolyzer to generate hydrogen [17–19]. The hydrogen will be stored in the hydrogen tanks and is later used by the fuel cell to meet the power shortage.

There are many studies in the literature of clean energy implementation concerning hydrogen storage for relatively smaller-scale applications (residential/office scale), similar to what was put forward by Silva et al. [20], where they discuss the techno-economic evaluation of a standalone photovoltaic-fuel cell battery system for power supply in an isolated community in Brazil. Battery banks were found to be a better option to store energy for solar power generation system as compared to their hydrogen counterpart. Dursun [21] investigated the feasibility of solar-fuel cell system employment to supply the electric demand of the Kirklareli University campus in Turkey. Levelized cost of energy for a standalone PV-fuel cell and its grid-connected counterpart was found to be \$1.051/kWh and \$0.293/kWh, respectively. Kalinci [22] performed a comparison investigation on alternative renewable energies to supply power in Bozcaada Island, Turkey. The levelized cost of energy for grid-wind and standalone wind-PV-fuel cell system was estimated to be \$0.103/kWh and \$0.836/kWh, respectively. Mason and Zweibel [23] studied the feasibility of replacing conventional gasoline-based trucks and vehicles with hydrogen ones. According to the results of their study, this replacement can cut the carbon emission by 90% and reduce primary energy significantly.

In addition to the battery storage problems, inability to meet the mine's total energy demand is another potential obstacle that prevents successful implementation of standalone renewable systems in mining industries. To supply a mine with 100% renewable energy, the energy system should be able to meet the mine's total energy demands, including all forms of electricity, haulage, and heating requirements. To the best of the authors' knowledge, this is the first study of an all-inclusive hybrid hydrogen-renewable storage energy system design which can be financially competitive with the conventional mine energy system (usually diesel-fueled). For this reason, the present paper, for the first time, offers a novel integrated renewable-multi storage (battery/fuel cell/thermal storage) solution to cover 100% off-grid mining power demands (including all forms of demands) as a standalone system. It offers a method for estimation of reduction in the carbon and other emissions, and detailed financial benefits of implementation of the proposed energy system.

2. Methodology

Two types of underground mining operations are addressed in this study: (1) underground (U/G) mines with minimal mineral process, and (2) U/G mines with intensive mineral process. According to Natural Resources Canada [24] every kiloton of ore hoisted costs ~131 MWh energy for a typical U/G mine with minimal mineral process. This figure rises up to ~174 MWh per kiloton for an U/G mine with intensive mineral process.

Figure 1 shows the comparative energy use for U/G mines. Generally, mine overall energy consumption can be subdivided into three types: electricity, haulage (motive power), and thermal energy. Among these, electricity represents a major portion of the consumed energy for both types of the mines with 65% for minimal and 73% for intensive mineral processing requirements. Motive power takes 20% and 16%, while the thermal load is 15% and 11% for minimal and intensive processing cases, respectively. These energy components have to be met by resources (such as grid, diesel-based system or renewable) available at the mine site. Throughout this paper, the subscripts E, M, and T are used to represent the variables associated with electricity, motive, and thermal power, respectively.

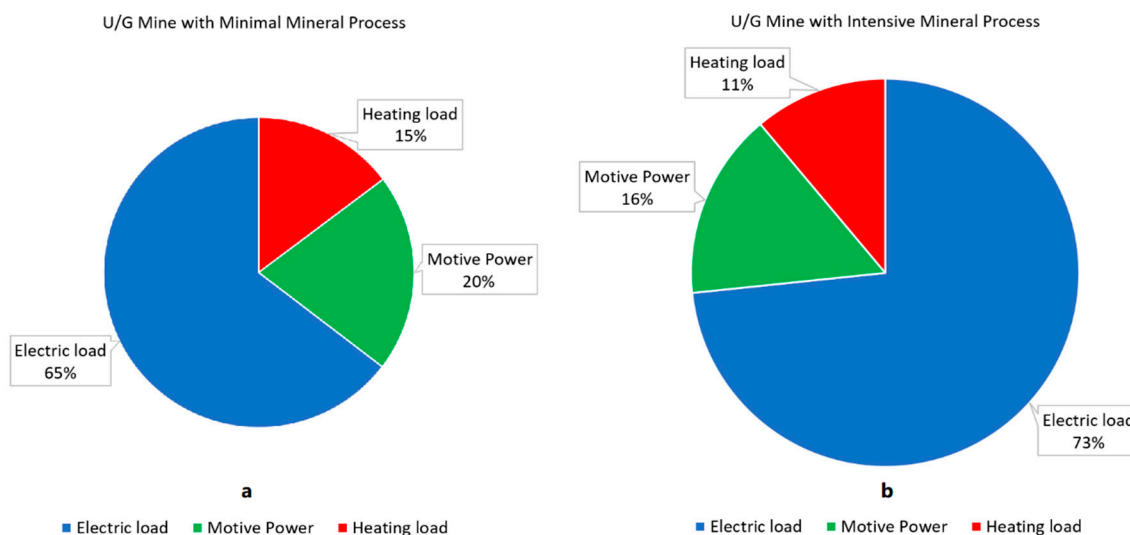


Figure 1. Comparative energy use for underground (U/G) mines: (a) U/G mining operation with minimal mineral process; (b) U/G mining operation with intensive mineral process [24].

2.1. Conventional Remote Mine Energy System

Remote mines are usually reliant on diesel fuel for their overall energy demands. Figure 2 shows the conventional design for remote mine energy systems. Diesel generators are used to supply the electric load. The energy required to run the generator is provided by diesel tank. The amount of diesel (in liter) and corresponding costs (US\$) can be calculated as follows [25]:

$$Q_{Di,E}(t) = \frac{P_E(t)}{HV_{Di} \times \rho_{Di} \times \eta_{Di,Gen}} \quad (1)$$

$$C_{Di,E}(t) = Q_{Di,E}(t) \times Pri_{Di} \quad (2)$$

where P_E , HV_{Di} , ρ_{Di} , and $\eta_{Di,Gen}$ represent mine electricity demand, diesel heating value, diesel density, and efficiency of diesel generator. Also, Pri_{Di} denotes the diesel price. In the conventional system, diesel trucks are used for haulage purposes. One can use the following equations to calculate the diesel amount to run the trucks and corresponding costs.

$$Q_{Di,M}(t) = \frac{P_M(t)}{HV_{Di} \times \rho_{Di} \times \eta_{Di,Tr}} \quad (3)$$

$$C_{Di,M}(t) = Q_{Di,M}(t) \times Pri_{Di} \quad (4)$$

where P_M and $\eta_{Di,Tr}$ represent mine motive power demand and trucks average efficiency. For mine heating demand, a heat recovery system from the diesel generators embedded in the system can partially meet requirements; the rest is provided by burning diesel.

$$Q_{Di,T}(t) = \frac{P_T(t) - P_E(t) \times (1 - \eta_{Di,Gen}) \times \eta_{hr,Gen}}{HV_{Di} \times \rho_{Di} \times \eta_{Di,bur}} \quad (5)$$

$$C_{Di,T}(t) = Q_{Di,T}(t) \times Pri_{Di} \quad (6)$$

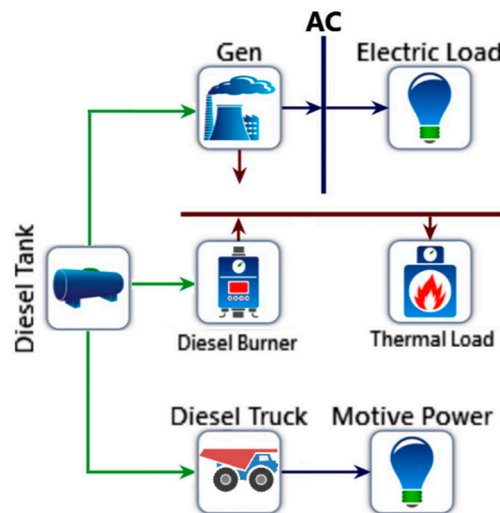


Figure 2. Diesel-based mine energy system configuration.

It is assumed that the generator converts the diesel energy to electricity with the efficiency of $\eta_{Di,Gen}$, and the remaining energy is rejected as heat. This heat can be recovered and returned to the system by heat recovery efficiency of $\eta_{hr,Gen}$.

Greenhouse Gases Emission

The emissions for any pollutant of p (carbon dioxide, carbon monoxide, unburned hydrocarbons, particulate matter, sulfur dioxide and nitrogen oxides) can be calculated over time, using the corresponding emission factor of each pollutant (EF_p) and amount of diesel consumption by the diesel-based components (L_{Di}) [25]:

$$EM_p(t) = \frac{L_{Di}(t)}{EF_p} \quad (7)$$

Considering the current levied carbon emission penalty (i.e., \$35/ton of CO₂) [26], the imposed tax is a sizable portion of the operating costs and needs to be embedded in the analysis. The emission taxes over time can be expressed as follows:

$$Tax_{em}(t) = EM_p(t) \times Pe_p \quad (8)$$

where Pe_p denotes the emission penalty (\$/t) for each pollutant of p .

2.2. Renewable Energy System Configuration

In the present study, an integrated renewable–multi storage system with six different configurations are proposed, and the techno-economical outcomes are compared with the conventional diesel-based energy system. Figure 3a–f show the configurations of the proposed systems, with the following details:

- Figure 3a represents the battery–fuel cell–hydrogen truck system (B/FC/HT). The wind farm is connected to AC bus to feed the electrical demand of the mine; the surplus power from wind farm is stored in battery banks or fed to the electrolyzer to generate hydrogen. Hydrogen is stored in the hydrogen tanks which feed the hydrogen trucks for haulage purposes and fuel cells to cover the power shortages to supply 100% of the load. Also, to supply the heating demand of the mine, thermal energy is stored in the thermal storage system using the surplus of the wind farm during low heat demand season, and it is used when the heating demand is peaked. Note that the thermal storage system is embedded in all of the configurations.
- Figure 3b illustrates the battery–hydrogen truck system (B/HT) configuration. In this system, the power shortage is covered by battery bank and there is no need for fuel cell; however, electrolyzers use surplus wind power to produce hydrogen which will be stored and used in hydrogen tanks.
- Figure 3c is the fuel cell–hydrogen truck system (FC/HT). In this case, all the power shortages are supplied by fuel cells, and there is no need for battery banks.
- The configuration of battery–fuel cell–battery electric truck system (B/FC/BET) is shown in Figure 3d. In this design, the electric load needs of the mine and the BET are both covered by hybridization of wind turbine, battery, and fuel cell. Also, to avoid equipment downtime (when the battery is under charge), battery swapping will be necessary, which means that for every truck, there is a spare battery pack.
- Figure 3e represents the battery–battery electric truck system (B/BET). Wind turbine combined with battery banks supply the electric load and battery electric trucks power, and there is no need for electrolyzer, hydrogen tank, and fuel cell in this system.
- The last one is the fuel cell–battery electric truck system (FC/BET), which is shown in Figure 3f. The electric load and motive power are supplied with wind turbine and fuel cell system. There is no need for a battery bank in this system.

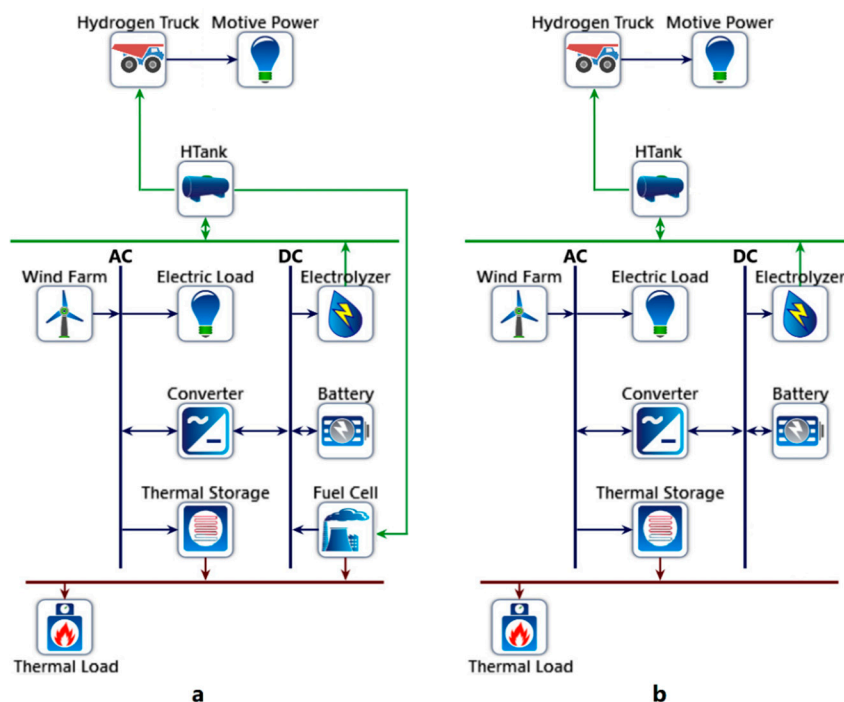


Figure 3. Cont.

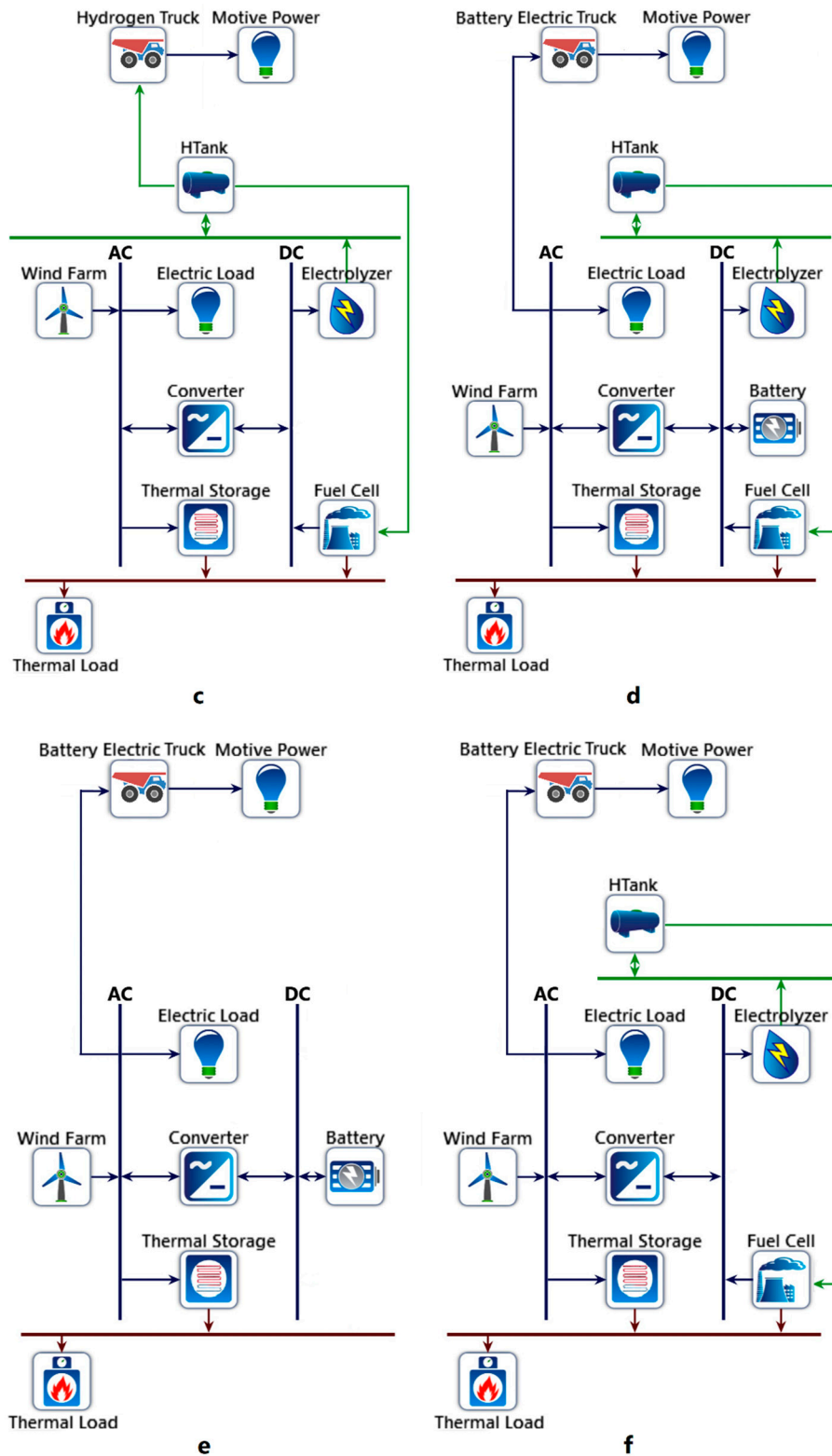


Figure 3. (a) Battery–fuel cell–hydrogen truck system; (b) battery–hydrogen truck system; (c) fuel cell–hydrogen truck system; (d) battery–fuel cell–battery electric truck system; (e) battery–battery electric truck system; (f) fuel cell–battery electric truck system.

2.3. Renewable Energy System

In the following subsection, the renewable systems mathematical model is presented. The proposed systems are all module-based designs. The module chosen for this study is a 1 MW size renewable system; meaning that the system can supply 1 MW of the mine's total energy demand (including all forms of electricity, haulage, and heating demands). All the calculations are based on the module size. The mine's modular sized annual energy demands are calculated using Figure 1 and are listed in Table 1.

Table 1. Mine modular sized annual energy demands.

Parameters	U/G Mining Operation with Intensive Mineral Process	U/G Mining Operation with Minimal Mineral Process
Electric demand	6430 MWh/y	5659 MWh/y
Motive power	1358 MWh/y	1805 MWh/y
Thermal demand	972 MWh/y	1296 MWh/y

The total number of modules required to run the mine with 100% renewable energy can be obtained by:

$$N_{modules} = \frac{P_{tot}}{P_{module}} \quad (9)$$

The modular design of the renewable system enables the decisionmakers to select modules in custom combinations, allowing them to choose only the required number of modules to run the mine with a partially renewable system.

2.3.1. Wind Turbine

Wind turbine is the primary source of energy in the proposed designs. The power generated by the wind turbine is determined by wind speed. Hourly wind speed ($V(t)$) data provided by the NASA Prediction of Worldwide Energy Resource [27] are incorporated into HOMER software [25] to calculate the output power in each time step. In this regard, a three-step process is used by HOMER [25]: 1. The wind speed is calculated at the hub height of the turbine; 2. The output power is calculated at standard air density using the hub height wind speed and turbine's power curve; and 3. The power output is adopted to the actual air density. One can calculate wind speed at the hub height by the following equation:

$$V_{hub} = V_{anem} \frac{\ln(z_{hub}/z_0)}{\ln(z_{anem}/z_0)} \quad (10)$$

where z_{anem} and V_{anem} represent the anemometer height and measured wind speed at this height. Also, z_{anem} and z_0 denote the hub height of the wind turbine and surface roughness length, respectively. One can calculate the wind turbine power output using a curve fitting technique [6,15]:

$$P_w(t) = \begin{cases} 0 & \text{if } V(t) < V_c \\ a_1 V^n(t) + \dots + b_1^2 V^2(t) + c_1 V(t) + d_1 & \text{if } V_c \leq V(t) < V_1 \\ a_2 V^n(t) + \dots + b_2^2 V^2(t) + c_2 V(t) + d_2 & \text{if } V_1 \leq V(t) < V_2 \\ a_3 V^n(t) + \dots + b_3^2 V^2(t) + c_3 V(t) + d_3 & \text{if } V_2 \leq V(t) < V_f \\ a_4 V^n(t) + \dots + b_4^2 V^2(t) + c_4 V(t) + d_4 & \text{if } V(t) > V_f \end{cases} \quad (11)$$

Here, V_c and V_f are the cut-in and cut-off wind speeds. In addition, V_1 and V_2 represent the intermediate speed values used to maximize the curve fitting accuracy. $P_w(t)$ is the power output at the standard pressure and temperature. The actual power output can be obtained using the following expression:

$$P_{w,ac}(t) = \left(\frac{\rho}{\rho_0}\right) P_w(t) \quad (12)$$

2.3.2. Battery Bank

Whenever the wind power generated is higher than the demand, the surplus power is stored in the battery bank. During the charging state, capacity of the battery bank can be estimated as follows [6,15]:

$$C_B(t) = C_B(t-1)(1-\sigma) + (P_{w,ac}(t) - P_L(t))\eta_{Batt} \quad (13)$$

where

η_{Batt} and σ are the charging efficiency of the battery bank and self-discharge rate of the battery bank, respectively. Moreover, $P_L(t)$ represents the electric load demand at the corresponding time which is equal to:

$$P_L(t) = \begin{cases} P_E(t) & \text{for the designs with hydrogen trucks} \\ P_E(t) + P_M(t) & \text{for the designs with battery electric trucks} \end{cases} \quad (14)$$

Whenever the wind power is lower than the demand, the power shortage should be ratified by battery bank. The discharge state capacity of the battery bank can be expressed as follows:

$$C_B(t) = C_B(t-1)(1-\sigma) + (P_L(t) - P_{w,ac}(t))\eta_{conv} \quad (15)$$

η_{conv} denotes the efficiency of the converter. Note that the battery bank charge capacity should be kept in the safe limits.

$$(1 - DOD)C_{Batt} \leq C_B(t) \leq C_{Batt} \quad (16)$$

where C_{Batt} and DOD are the battery bank nominal capacity and discharge maximum depth, respectively.

2.3.3. Electrolyzer

The electrolyzer is an electrochemical system which utilizes the surplus power from the wind turbine to generate hydrogen through the water electrolysis process. One can calculate the amount of generated hydrogen, in kg, as follows [28]:

$$M_{H_2,gen}(t) = \frac{(P_{w,ac}(t) - P_L(t))\eta_{conv}}{\eta_{elec} \times HV_{H_2} / \rho_{H_2}} \quad (17)$$

In Equation (17), η_{elec} , HV_{H_2} , and ρ_{H_2} are the electrolyzer efficiency, hydrogen heating value, and density of hydrogen, respectively.

2.3.4. Fuel Cell

As mentioned before, a fuel cell is used to cover the power shortage in case of wind turbine/battery failure to supply full electric load. The power generation by fuel cell can be expressed by [28,29]:

$$P_{FC}(t) = M_{H_2,cons}(t)\eta_{FC} \frac{HV_{H_2}}{\eta_{conv} \times \rho_{H_2}} \quad (18)$$

where η_{FC} represents the fuel cell efficiency.

2.3.5. Thermal Storage System

As indicated in Table 1, heating demands for U/G mining operations with minimal and intensive mineral process are 972 MWh/y and 1296 MWh/y, respectively. Heating is a seasonal demand and it is not distributed evenly throughout the operating year. Using the heating degree days (HDD) value at the mine site location [30], the distribution of mine thermal demands over an operating year is calculated. Figure 4 shows the monthly heating demand of U/G mining operations. As illustrated in this figure, January, February, March, and December account for the major portion of heating demand.

On the other hand, there is almost no heating required during the summer season (June–August). Mine heating systems are mostly designed based on the peak loads and worst climate conditions at the mine site. Given the wind power generation volatility, provision of this heat from direct wind electricity imposes significant capital investments and operational expenditures to the mine. On the other hand, the seasonal thermal storage system can help resolve this issue by downsizing the renewable power generation system. In this regard, a rock-pile based seasonal thermal energy storage with the capacity equal to the quarter of mine annual heating load is selected for this study. This would guarantee a sufficient amount of heating provision to the mine, even though there are no winds for weeks. One can calculate the thermal storage capacity during the charging and discharge state by:

$$C_{TS}(t) = \begin{cases} C_{TS}(t-1)\eta_{TS} + (P_{w,ac}(t) - P_L(t))\eta_{ET, conv} & \text{Charging state} \\ C_{TS}(t-1)\eta_{TS} - P_T(t) & \text{Discharge state} \end{cases} \quad (19)$$

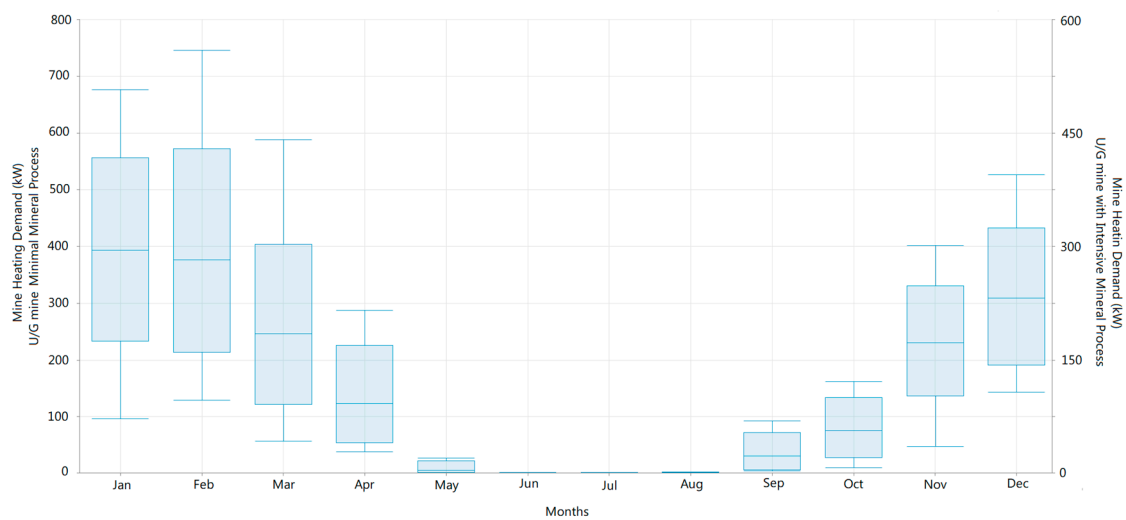


Figure 4. Monthly heating demand of the mine.

The thermal storage charge capacity should be kept between the limits:

$$C_{TS,min} \leq C_{TS}(t) \leq C_{TS,nom} \quad (20)$$

2.4. Economic and Financial Calculations

The net present cost (NPC) of a system represents the present value of all the costs, which includes installation, operating and maintenance, replacement and fuel costs, and emission penalties throughout the lifetime of the project, reduced by all the revenues and present value earned during this time. One can calculate the NPC of the system using the following equation, where R_y and N represent the net cash flow in year y and lifetime of the project, respectively [25,31].

$$NPC = \sum_{y=0}^N \frac{R_y}{(1+i)^y} \quad (21)$$

Also, i is the real discount rate (%), which can be expressed as follows [25]:

$$CRF = \frac{i' - f}{1 + f} \quad (22)$$

where i' and f are the nominal discount rate and expected inflation rate.

The levelized cost of energy (COE) can be defined as the average cost per unit of mine total energy for which the investment just breaks even.

$$\text{COE} = \frac{\text{NPC} \times \text{CRF}}{\sum_{t=0}^{N \times 8760} (P_E(t) + P_M(t) + P_T(t)) \Delta t} \quad (23)$$

Here, CRF represents the capital recovery factor, which is calculated using:

$$\text{CRF} = \frac{i(1+i)^N}{(1+i)^N - 1} \quad (24)$$

2.5. Simulation and Optimization

The hybrid optimization of Multiple Energy Resources (HOMER) Software [25] coupled with a developed spreadsheet integrated software are used for both the conventional and standalone renewable systems simulation and the optimization. The optimization is based on the lowest total net present cost [25] in which the user-specified characteristics are met with the system configuration. The parameters used for the simulations are listed in Table 2. Here, it should be pointed out that all the prices used for the financial evaluation are in US dollars.

Table 2. The system component parameters.

Parameters	Value	Ref	Parameters	Value	Ref
Nominal discount rate (i')	8%	[32]	Inflation rate (f)	2%	[32]
Fuel Cell capital cost (\$/kW)	1344	[33]	Fuel Cell replacement cost (\$/kW)	1070	[33]
Battery capital cost (\$/kWh)	500	[15]	Battery replacement cost (\$/kWh)	400	[15]
Diesel Truck capital cost (\$/kW)	1139	[33]	Diesel Truck replacement cost (\$/kW)	1139	[33]
H Truck capital cost (\$/kW)	1709	[33,34]	H Truck replacement cost (\$/kW)	1709	[33,34]
BE Truck capital cost (\$/kW)	1709	[33,34]	BE Truck replacement cost (\$/kW)	1709	[33,34]
Electrolyzer capital cost (\$/kW)	1100	[35,36]	Electrolyzer replacement cost (\$/kW)	825	[35,36]
H Tank capital cost (\$/kW)	1000	[35]	H Tank replacement cost (\$/kW)	750	[35]
Wind turbine capital cost (\$/kW)	2606	*	Wind turbine replacement cost (\$/kW)	2606	*
Lifetime of the mine (years)	20	-	Fuel Cell efficiency	0.5	[37]
Electrolyzer efficiency	0.75	[38,39]	Convertor efficiency	0.95	[15]
Lifetime of fuel cell (years)	5	[37]	Lifetime of battery (years)	15	[15]
Lifetime of H Truck (years)	5	[33,34]	Lifetime of Diesel Truck (years)	4	[33]
Lifetime of BE Truck (years)	5	[33,34]	Lifetime of Electrolyzer (years)	10	[36]
Lifetime of Turbine (years)	20	[40]	Lifetime of Convertor (years)	15	[15]
Lifetime of Tank (years)	20	[37]	Diesel price (\$/L)	0.81	[41]
Diesel generator replacement cost (\$/kW)	500	[15]	Diesel generator cost (\$/kW)	500	[15]
Carbon tax (\$/ton)	35	[25]	Thermal storage system cost (\$/MWh)	544.72	[42]
Convertor replacement cost (\$/kW)	300	[15]	Convertor capital cost (\$/kW)	300	[15]

* The prices for wind turbine are based on a real-life mining operation report which asked to be anonymous in delivery of this investigation.

3. Results

Results of this study are delivered in three different stages. Throughout the first stage, financial-environmental results of the diesel-based system will be presented. In the second stage, results of the proposed renewable systems concerning the introduced case study will be brought and compared to find the financially-feasible solutions for an energy system of the given underground mining operation.

In the last stage of this section, results of the parametric study, in order to globalize the results of the proposed systems, will be presented.

3.1. Case Study

To introduce the concept in a more elaborate and realistic way, an underground Canadian mine, Diavik Diamond Mine, located in the Northwest Territories, is selected. To evaluate feasibility of the standalone renewable system, local wind speed and ambient temperature data was needed for the case introduced. Accordingly, NASA Prediction of Worldwide Energy Resource [27] and Canadian Weather, Climate and Hazard [30] databases were referred to retrieve local wind speed and ambient temperature data, respectively. Figure 5 shows the hourly basis wind speed data at the mine location.

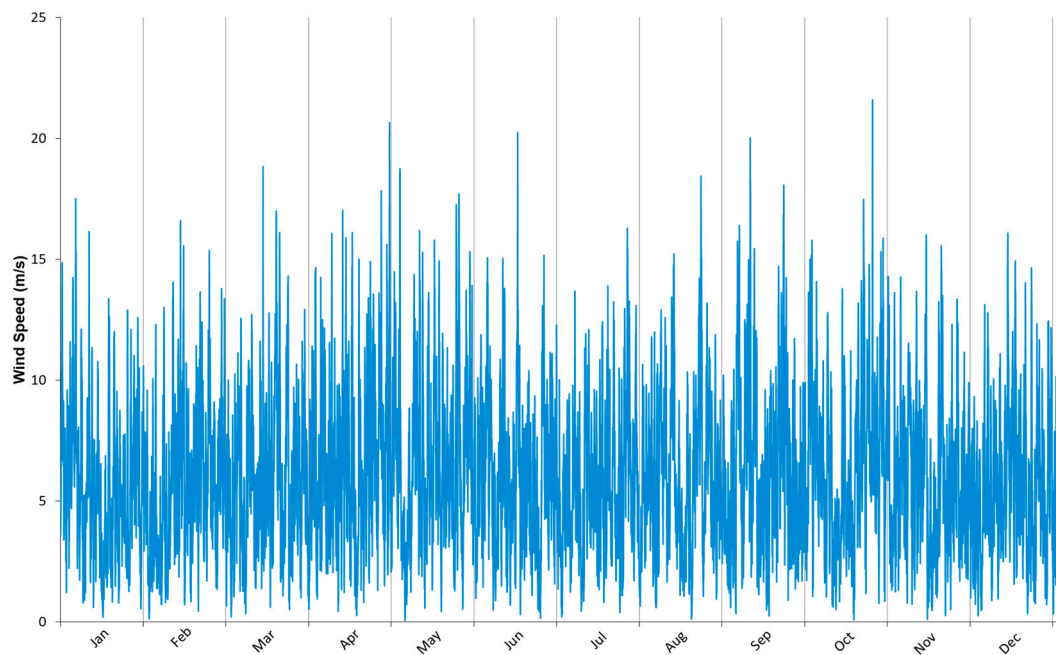


Figure 5. Historical wind speed hourly data [27].

3.2. Diesel-Based System Results

In order to have a wider spectrum of financial results of the diesel-based energy case, the system was tested under various scenarios for both the mining operations with intensive and minimal processes. Figure 6 shows the energy cost associated with the diesel-based energy system with various diesel prices and levied carbon taxes. As depicted in Figure 6, with the current diesel market price and carbon emission penalty (\$0.81/L and \$35/t), every kWh of mine total energy costs \$0.37. Results of the simulations show that this figure can rise up to \$0.5/kWh with increasing the diesel price and carbon emission penalty. According to the results of simulations, haulage is more cost-intensive compared to the other two forms of mine energy use in diesel-based mining operations. Hence, the higher the haulage portion in the mine total energy consumption, the higher the cost of energy. Therefore, one unit of energy should cost more for a mine with minimal process plant, as its portion of haulage is higher. However, heat recovery from the diesel generators offers a significant financial benefit to the mining operations with higher portion of thermal demands, by recovering a considerable amount of heat from generators. This explains the higher relative cost of energy for the U/G mine with intensive mineral process.

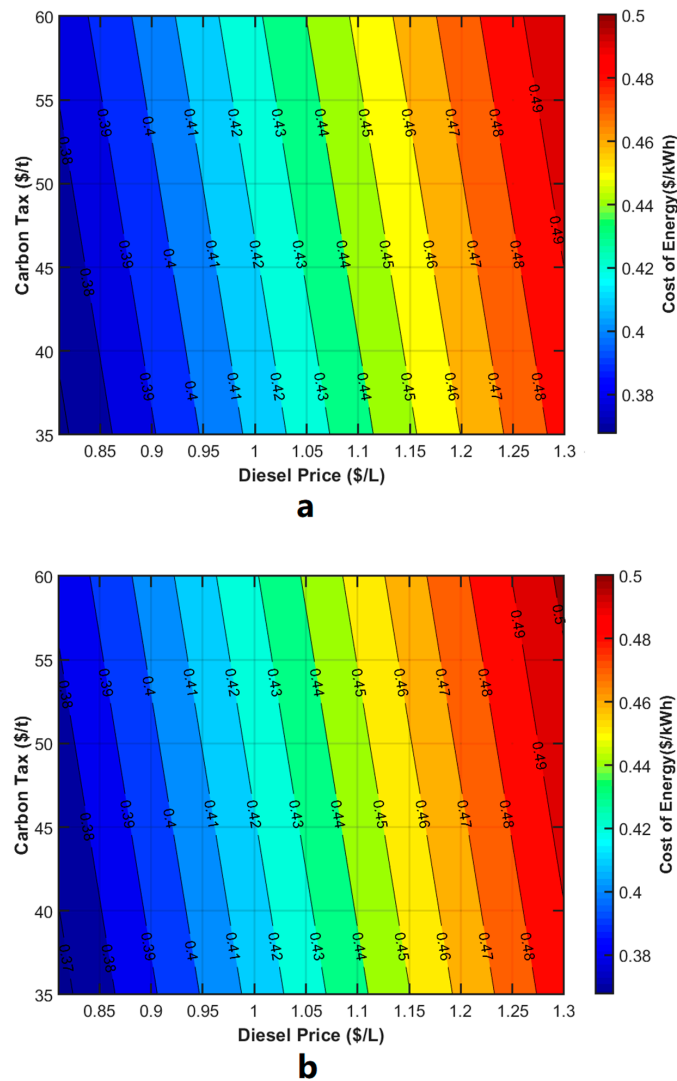


Figure 6. Comparative energy use for U/G mines: (a) U/G mining operation with minimal mineral process; (b) U/G mining operation with intensive mineral process.

In addition, Table 3 summarizes the different pollutant emissions caused by the conventional diesel-based energy system. As shown in this table, more than 5 kilotons of CO₂ is emitted by this system annually for every MW of mine power. Note that these calculated emissions will be scaled up by multiplying it by the size of the mine’s overall power. For example, a 10 MW-sized mining operation has 10 times higher emissions. Aside from its environmental impacts, given the national government’s plans to gradually escalate carbon taxes, these emissions will impose a considerable financial burden to the mining operation.

Table 3. Pollutant emissions of the diesel-based system for every MW of mine total power.

Type of the Mine	U/G Mining Operation with Minimal Mineral Process	U/G Mining Operation with Intensive Mineral Process	Units
Pollutant			
Carbon Dioxide	5292.625	5499.787	t MW ⁻¹ y ⁻¹
Carbon Monoxide	33.362	34.667	t MW ⁻¹ y ⁻¹
Unburned Hydrocarbons	1.456	1.513	t MW ⁻¹ y ⁻¹
Particulate Matter	0.202	0.21	t MW ⁻¹ y ⁻¹
Sulfur Dioxide	12.96	13.468	t MW ⁻¹ y ⁻¹
Nitrogen Oxides	31.34	32.867	t MW ⁻¹ y ⁻¹

3.3. Renewable System Results

Table 4 summarizes the optimal sizing of the six previously indicated renewable systems. Also, Table 4 provides the financial costs associated with implementation of proposed renewable energy systems for both types of the mines. Each scenario is individually simulated to find the optimum financial option based on the lowest total net present cost.

Table 4. Comparison of the economic results of different renewable energy systems.

Type of the Mine	U/G Mining Operation with Minimal Mineral Process					
	B/FC/BET	B/BET	FC/BET	B/FC/HT	B/HT	FC/HT
Wind Turbine (MW)	2	4	3	2	4	3
Battery (MWh)	1	5	–	1	5	–
Fuel Cell (MW)	0.5	–	1	0.5	–	1
Electrolyzer (MW)	2	1	2	2	1	2
H Truck (kW)	–	–	–	412	412	412
BE Truck (kW)	412	412	412	–	–	–
CAPEX (M\$)	19.1	25.7	19.3	25.9	27.2	27.2
COE (\$/kWh)	0.28	0.35	0.29	0.35	0.37	0.39
Payback (years)	10.7	18.2	11.5	18.4	21.1	24.1
Type of the Mine	U/G Mining Operation with Intensive Mineral Process					
	B/FC/BET	B/BET	FC/BET	B/FC/HT	B/HT	FC/HT
Wind Turbine (MW)	2	4	3	2	4	3
Battery (MWh)	1	5	–	1	5	–
Fuel Cell (MW)	0.5	–	1	0.5	–	1
Electrolyzer (MW)	2	1	2	2	1	2
H Truck (kW)	–	–	–	310	310	310
BE Truck (kW)	310	310	310	–	–	–
CAPEX (M\$)	18.9	28.8	20.2	23.2	26	24.8
COE (\$/kWh)	0.27	0.37	0.30	0.30	0.35	0.34
Payback (years)	10.3	21.3	12.7	13.3	17.3	16.8
Feasibility Collar	Feasible		Poorly Feasible		Infeasible	

The feasibility status of each scenario is highlighted with certain colors. It is important to note that the present study is conducted for an underground mining operation with 20 years of expected lifetime. Therefore, life of the mine has a key role in designating the feasibility regions shown in Table 4. In this regard, the renewable systems with payback periods less than 15 years (contributing more than 25% of the mine lifetime) are deemed as “feasible”. However, 15 years of payback (75% of mine lifetime) is usually deemed as “poorly feasible”. Clearly, systems that pay back beyond the mine lifetime are marked as “infeasible”.

Here, it is shown that the hydrogen storage system provides comparably faster paybacks, due to its relatively lower capital expenditures (CAPEX) compared to the battery storage system. Results of this study demonstrate that, while very high fluctuated wind power generation conditions are strongly in favor of the fuel cell storage system, the battery storage system is more suitable for fast-balance response. This is because batteries are ideal for short-term small-scale storage and discharge, whereas the hydrogen offers long-term large-scale storage solutions. However, as in the real case scenario, wind generation power oscillates between these two conditions from time to time, and the combination of battery/hydrogen storage yields the optimum solution as highlighted in Table 4.

Moreover, as Table 4 shows, more feasible scenarios can be found in the mine with intensive mineral process. This can be related to motive power impact on the economics of the system. Similar to the diesel-based system, motive power is more cost-intensive, as compared to electricity and heat for mining operations powered by 100% renewable energy system. Therefore, a larger portion of haulage in mine total energy results in higher COE, and thus decreases the chances of successful renewable systems implementation.

3.4. Sensitivity Analysis Results

To have a wider spectrum of the feasibility of the proposed renewable system implementation for other cases, a parametric study was conducted, analyzing wind speed and market price impacts on the economics of the mine energy system. Figures 7 and 8 show the wind speed impact on the economics of the system. Accordingly, faster wind speeds are in favor of wind power generation systems. As seen in these figures, economics of the renewable system is highly sensitive to the average wind speed at the mine site location. With the current market prices, for average wind speeds lower than 5.5 m/s, the proposed renewable system is hardly feasible for remote mines with intensive mineral process, as its payback periods are 15 years or beyond. The threshold wind speed for the mines with minimal mineral process is 6 m/s. Consequently, before any implementation, a comprehensive research needs to be undertaken to make sure that the wind speed is high enough for such a renewable system deployment.

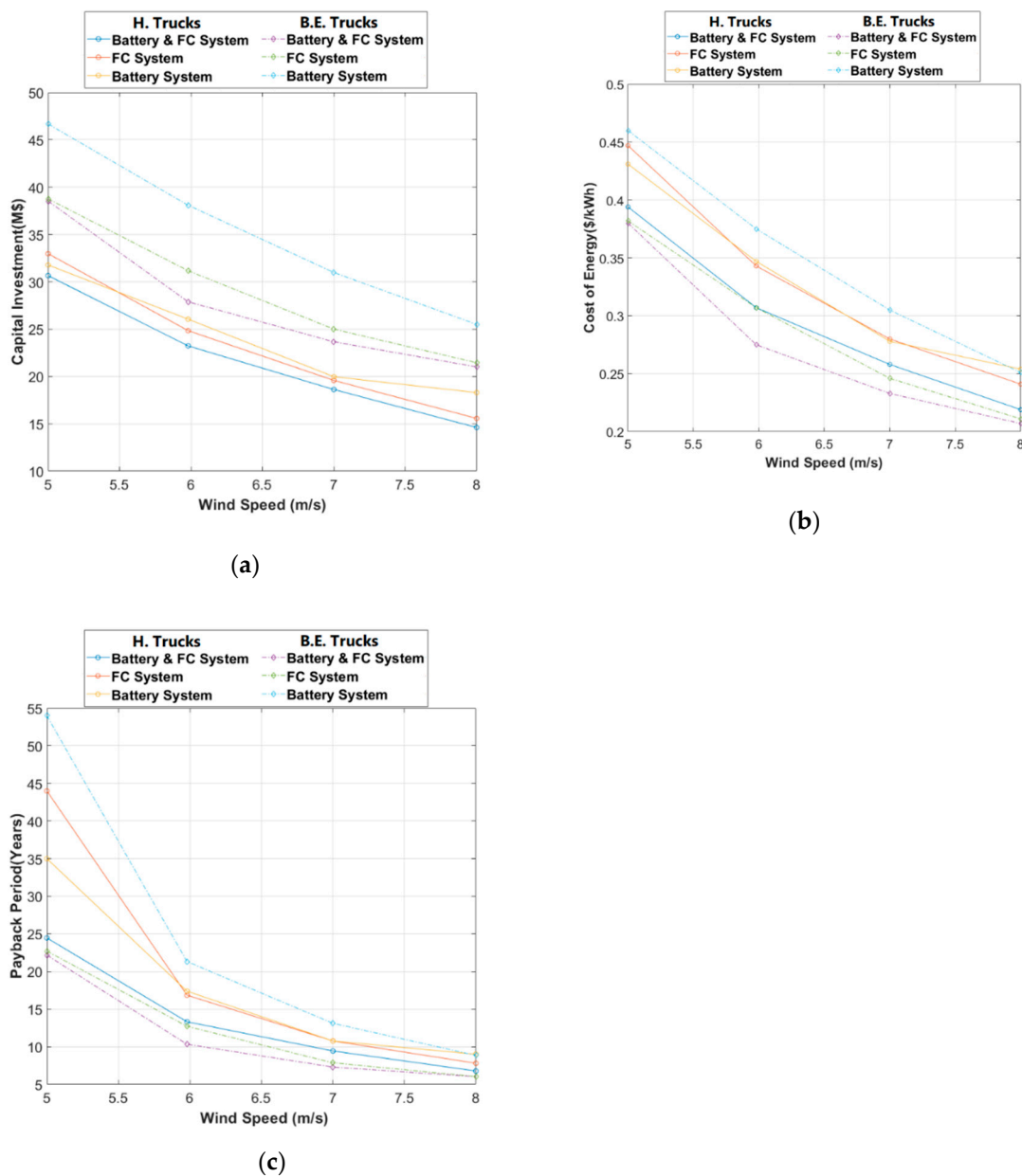


Figure 7. Wind speed effect on the economics of renewable system for U/G mining operation with intensive mineral process: (a) capital investment; (b) cost of energy; (c) payback period.

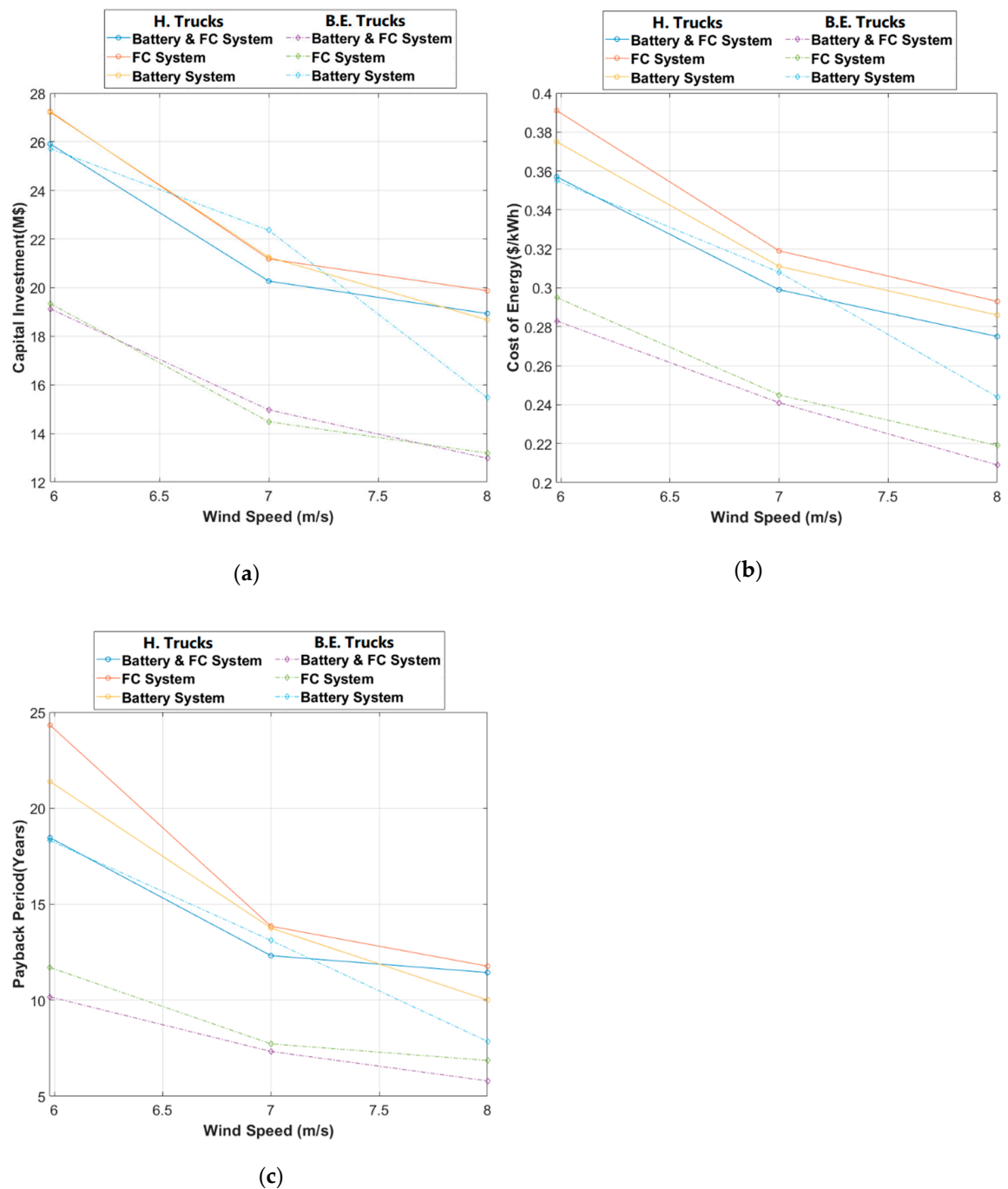


Figure 8. Wind speed effect on the economics of renewable system for U/G mining operation with minimal mineral process: (a) capital investment; (b) cost of energy; (c) payback period.

Note that the optimizations are performed for each case of different wind speeds individually, therefore the corresponding renewable systems may have different configurations.

The global renewable energy market is highly volatile, and costs of technologies have a high tendency to change over time. This study is based on the most up-to-date available information, and its results are derived based on current market prices. However, it can be predicted that technology prices may change. Therefore, it is important to perform a sensitivity analysis to evaluate the impacts of battery and fuel cell prices and their volatility. Accordingly, to better examine the effects of battery price variation, the simulations were run with different prices varying from the original value to 20% of the current market price, using the cost multiplier term. Figures 9 and 10 depict the battery price effect

on the economics of the renewable energy system. Accordingly, battery price has the most significant impact on B/HT and B/BET, by reducing their payback period by ~50%.

Similarly, different fuel cell prices are compared in Figures 11 and 12. If the fuel cell price decreases by 50%, most of the studied scenarios could be considered as feasible for implementation. It is also worth mentioning that B/FC/HT and B/FC/BET economics are more sensitive to the fuel cell price variation, as compared to its battery counterpart.

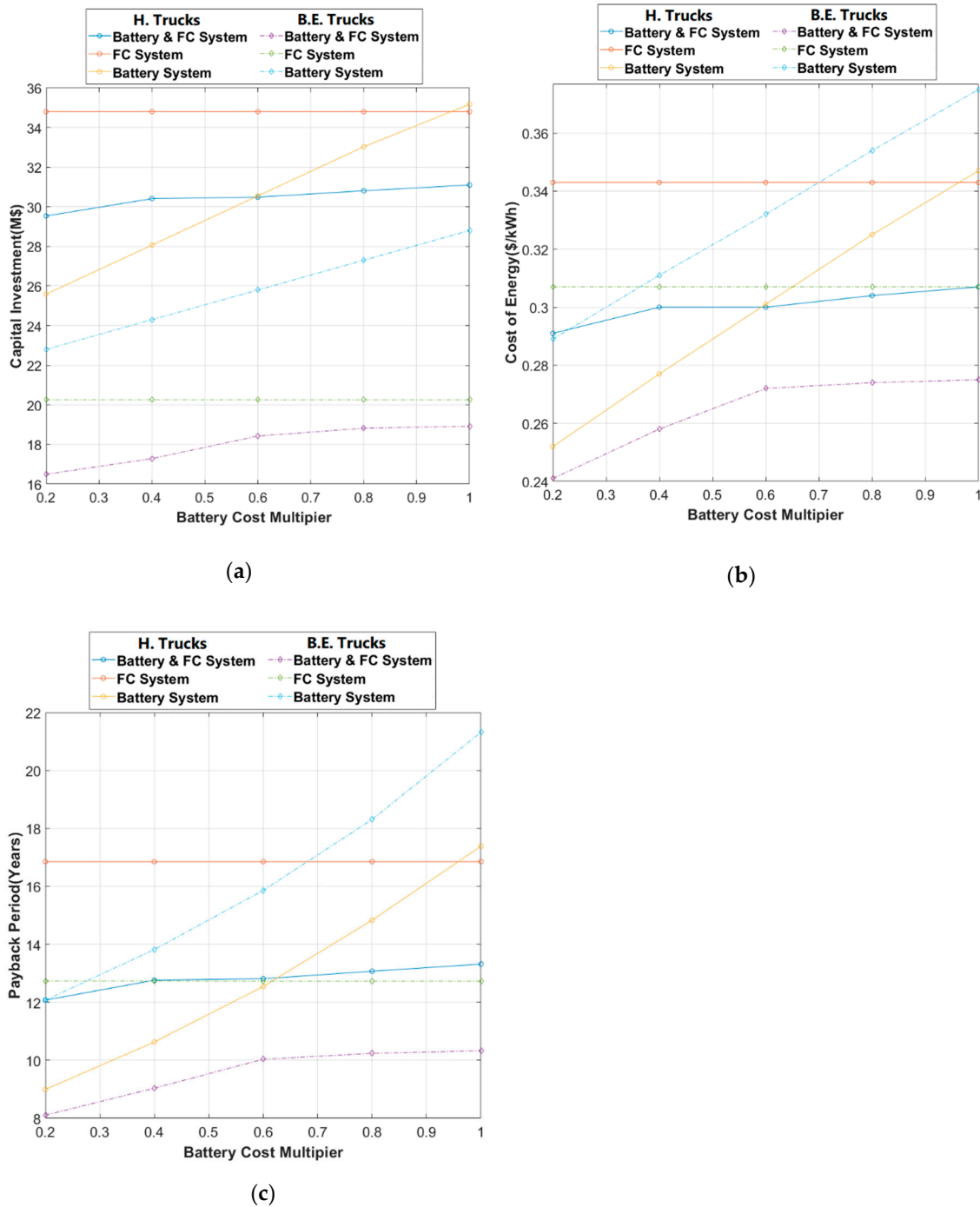


Figure 9. Battery price effect on the economics of renewable system for U/G mining operation with intensive mineral process: (a) capital investment; (b) cost of energy; (c) payback period.

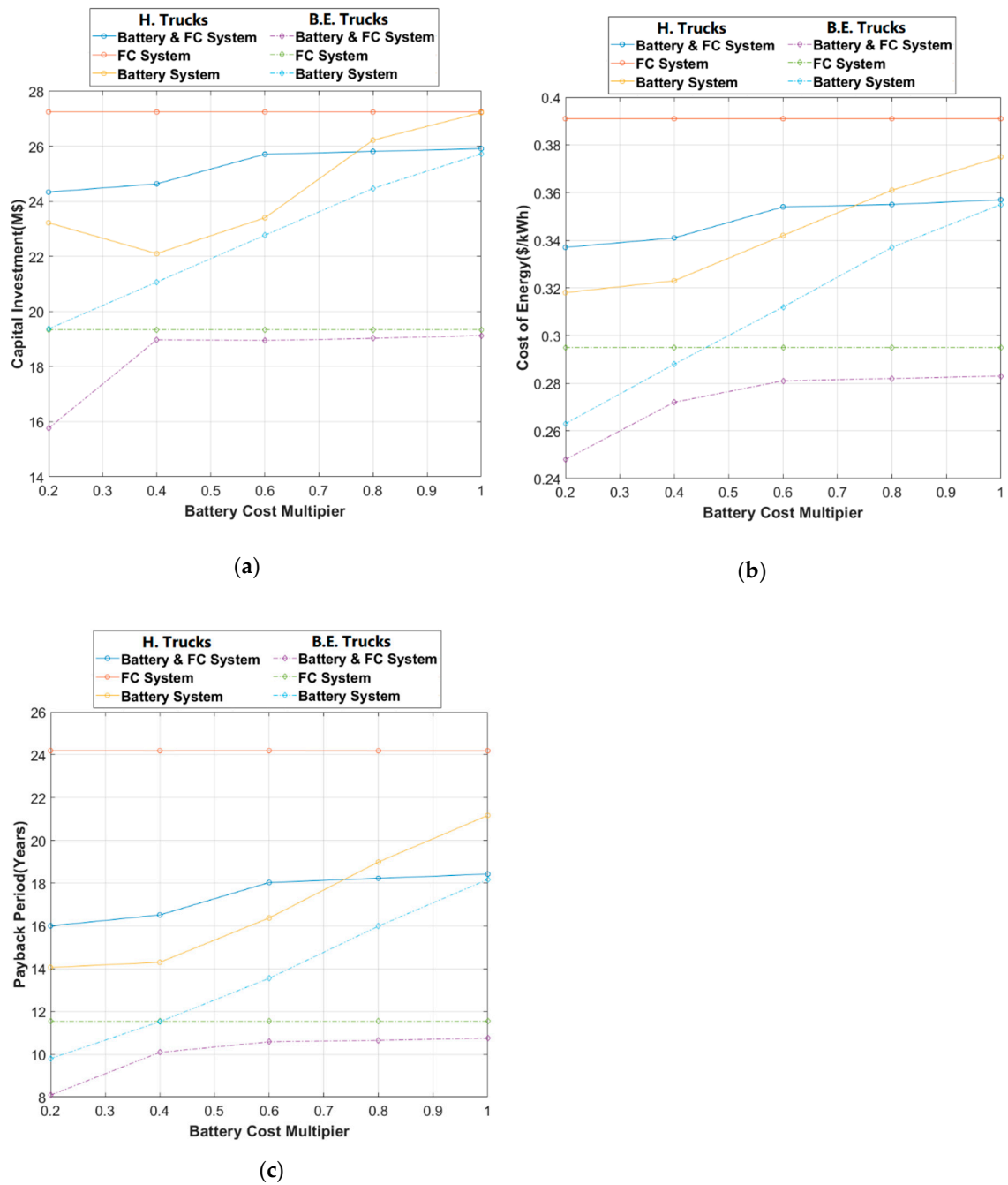


Figure 10. Battery price effect on the economics of renewable system for U/G mining operation with minimal mineral process: (a) capital investment; (b) cost of energy; (c) payback period.

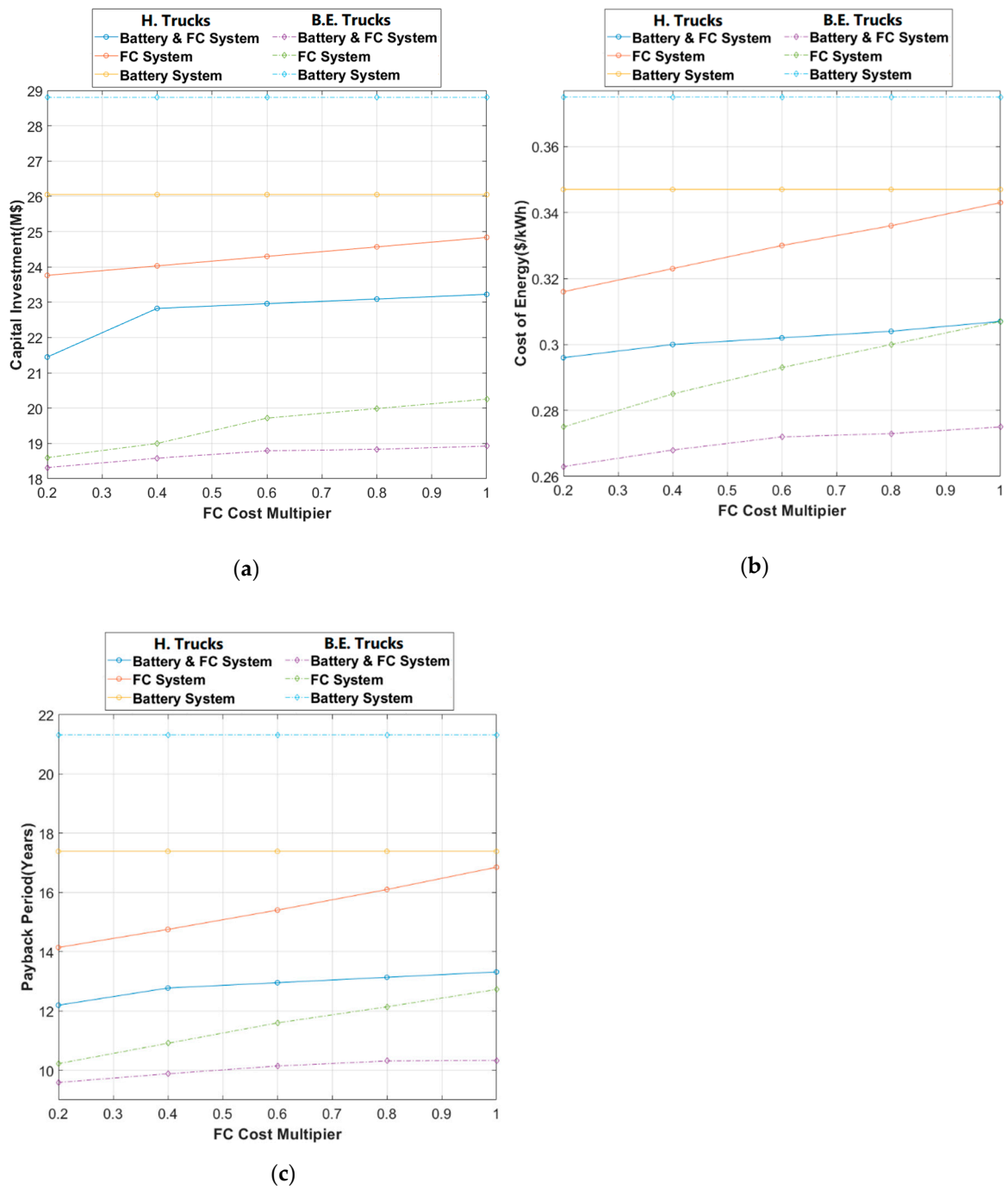


Figure 11. Fuel cell price effect on the economics of renewable system for U/G mining operation with intensive mineral process: (a) capital investment; (b) cost of energy; (c) payback period.

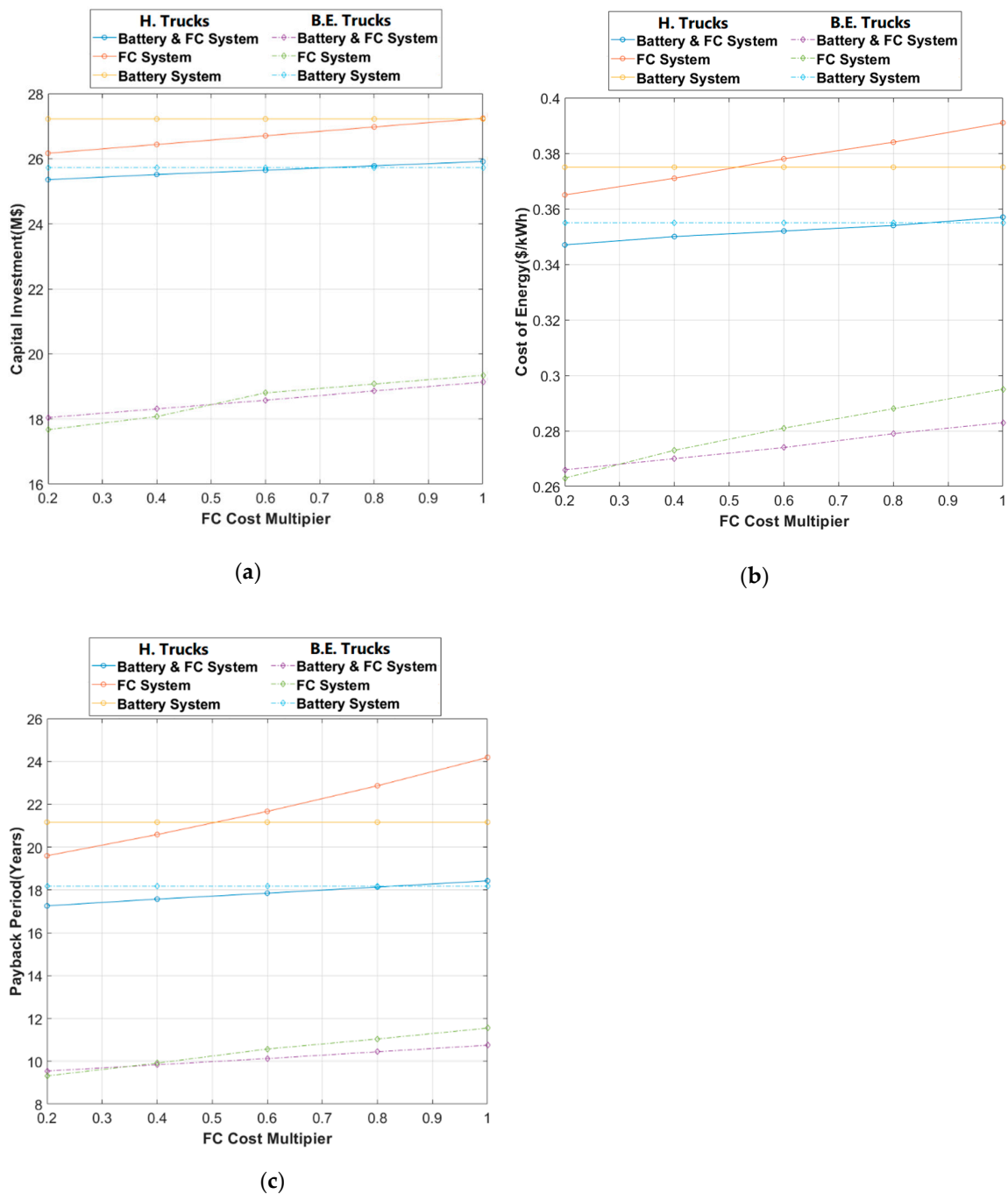


Figure 12. Fuel cell price effect on the economics of renewable system for U/G mining operation with minimal mineral process: (a) capital investment; (b) cost of energy; (c) payback period.

Results of the parametric study show that, although some of the proposed renewable systems are not recommended for implementation with the current market prices, they will become more feasible in the long term, as the financial burden of such technologies lessen by the time. In addition, it is worthwhile to notice that costs of diesel energy are expected to rise, due to pending escalations of carbon taxes which will yield in shorter payback years for the alternative renewable systems.

4. Conclusions

In this study, the feasibility of hybrid renewable–hydrogen energy systems for application in remote underground mines was investigated. A novel integrated renewable–thermal storage

solution was proposed. Comprehensive techno-economic evaluations were conducted to find the feasible scenarios. Throughout this study, some significant observations were made concerning employment of modular-based standalone renewable systems.

Despite high upfront costs, some of the proposed designs show promising prospects with regards to the cost of energy and payback period. However, life of the mine is a major factor in feasibility of the system, which should be taken into account prior to any site implementation.

According to the results of the simulations and optimizations, the combination of battery and fuel cell as an energy storage system yields better financial returns compared to only-battery and only-fuel cell systems. Also, electric trucks show more desirable results compared to their hydrogen counterparts, as they do not involve deficiencies of hydrogen generation process. The B/FC/BET system was found to be the most favorable option.

The potential carbon savings are deemed to be significant (more than 5000 tons per year for every MW of mine energy). Given the pending escalations of carbon taxes in the future, the removal of these greenhouse gas emissions will bring in considerable financial benefits.

Author Contributions: Conceptualization, H.K., S.A.G.-M. and A.P.S.; methodology, H.K.; software, H.K.; validation, H.K., S.A.G.-M. and A.P.S.; formal analysis, H.K.; investigation, H.K.; resources, H.K., S.A.G.-M. and A.P.S.; data curation, H.K.; writing—original draft preparation, H.K.; writing—review and editing, H.K., S.A.G.-M. and A.P.S.; visualization, H.K., S.A.G.-M. and A.P.S.; supervision, S.A.G.-M. and A.P.S. All authors have read and agreed to the published version of the manuscript.

Funding: This research received no external funding.

Conflicts of Interest: The authors declare no conflict of interest.

References

- Ghoreishi-Madiseh, A.S.; Kalantari, H.; Kuyuk, A.F.; Sasmito, A.P. A new model to analyze performance of mine exhaust heat recovery systems with coupled heat exchangers. *Appl. Energy* **2019**, *256*, 113922. [CrossRef]
- Kalantari, H.; Ghoreishi-Madiseh, S.A.; Amiri, L.; Sasmito, A.P.; Hassani, F. Numerical study of waste heat recovery by direct heat exchanger systems. *E&ES* **2020**, *463*, 012031.
- Natural Resources Canada. Energy Sources and Distribution. Available online: <https://oee.nrcan.gc.ca/corporate/statistics/neud/dpa/showTable.cfm?type=CP§or=agg&juris=ca&rn=3&page=6> (accessed on 22 May 2020).
- Ghoreishi-Madiseh, S.A.; Kuyuk, A.F.; Kalantari, H.; Sasmito, A.P. Ice versus battery storage; a case for integration of renewable energy in refrigeration systems of remote sites. *Energy Procedia* **2019**, *159*, 60–65. [CrossRef]
- Hongxing, Y.; Wei, Z.; Chengzhi, L. Optimal design and techno-economic analysis of a hybrid solar–wind power generation system. *Appl. Energy* **2009**, *86*, 163–169.
- Diaf, S.; Daif, D.; Belhamel, M.; Haddidi, M.; Louche, A. A methodology for optimal sizing of autonomous hybrid PV/wind system. *Energy Policy* **2007**, *35*, 5708–5718. [CrossRef]
- Nfah, E.M.; Ngundam, J.M.; Tschinda, R. Modelling of solar/diesel/battery hybrid power systems for far-north Cameroon. *Renew. Energy* **2007**, *35*, 832–844. [CrossRef]
- Nfah, E.M.; Ngundam, J.M. Modelling of wind/Diesel/battery hybrid power systems for far North Cameroon. *Energy Convers. Manag.* **2008**, *49*, 1295–1301. [CrossRef]
- Finding Data to Run HOMER. Available online: https://www.homerenergy.com/products/pro/docs/latest/finding_data_to_run_homer.html (accessed on 22 May 2020).
- Canadian Mining and Energy, Sustainability and Environment. Available online: https://www.miningandenergy.ca/sustainability/article/diavik_diamond_mine_turns_to_wind/ (accessed on 22 May 2020).
- Natural Resources Canada. Science and Data. Available online: <https://www.nrcan.gc.ca/science-and-data/funding-partnerships/funding-opportunities/current-investments/glencore-raglan-mine-renewable-electricity-smart-grid-pilot-demonstration/16662> (accessed on 22 May 2020).
- GLENCORE Canada. Raglan Mine. Available online: <https://www.glencore.ca/en/Media-and-insights/Insights/Raglan-Mine-Operates-its-Second-Wind-Turbine> (accessed on 22 May 2020).

13. Hlal, M.I.; Ramachandaramurthy, V.K.; Sarhan, A.; Pouryekt, A.; Subramaniam, U. Optimum battery depth of discharge for off-grid solar PV/battery system. *J. Energy Storage* **2019**, *26*, 100999. [CrossRef]
14. Salkuti, S.R. Comparative analysis of electrochemical energy storage technologies for smart grid. *TELKOMNIKA* **2020**, *18*, 2118–2124. [CrossRef]
15. Al-Sharafi, A.; Sahin, A.Z.; Ayar, T.; Yilbas, B.S. Techno-economic analysis and optimization of solar and wind energy systems for power generation and hydrogen production in Saudi Arabia. *Renew. Sustain. Energy Rev.* **2017**, *69*, 33–49. [CrossRef]
16. Shiroudi, A.; Taklimi, S.R.H.; Mousavifar, S.A.; Taghipour, P. Stand-alone PV-hydrogen energy system in Taleghan-Iran using HOMER software: Optimization and technoeconomic analysis. *Environ. Dev. Sustain.* **2013**, *15*, 1389–1402. [CrossRef]
17. Bansal, S.; Zong, Y.; You, S.; Mihet-Popa, L.; Xiao, J. Technical and Economic Analysis of One-Stop Charging Stations for Battery and Fuel Cell EV with Renewable Energy Sources. *Energies* **2020**, *13*, 2855. [CrossRef]
18. Cecilia, A.; Carroquino, J.; Roda, V.; Costa-Castelló, R.; Barreras, F. Optimal energy management in a standalone microgrid, with photovoltaic generation, short-term storage, and hydrogen production. *Energies* **2020**, *13*, 1454. [CrossRef]
19. Singh, S.; Chauhan, P.; Aftab, M.A.; Ali, I.; Hussain, S.M.; Ustun, T.S. Cost Optimization of a Stand-Alone Hybrid Energy System with Fuel Cell and PV. *Energies* **2020**, *13*, 1295. [CrossRef]
20. Silva, S.B.; Severino, M.M.; de Oliveira, M.A.G. A stand-alone hybrid photovoltaic, fuel cell and battery system: A case study of Tocantins, Brazil. *Renew. Energy* **2013**, *57*, 384–389. [CrossRef]
21. Dursun, B. Determination of the optimum hybrid renewable power generating systems for Kavakli campus of Kirklareli University, Turkey. *Renew. Sustain. Energy Rev.* **2012**, *16*, 6183–6190. [CrossRef]
22. Kalinci, Y. Alternative energy scenarios for Bozcaada island, Turkey. *Renew. Sustain. Energy Rev.* **2015**, *45*, 468–480. [CrossRef]
23. Mason, J.E.; Zweibel, K. Baseline model of a centralized pv electrolytic hydrogen system. *Int. J. Hydrogen Energy* **2007**, *32*, 2743–2763. [CrossRef]
24. Natural Resource Canada, Office of Energy Efficiency. Table 3: Secondary Energy Use and GHG Emissions by Industry. Available online: <https://www.nrcan.gc.ca/energy-efficiency/energy-efficiency-industry/energy-management-industry/energy-benchmarkingindustry/benchmarking-guides/5171#l> (accessed on 22 May 2020).
25. HOMER (Hybrid Optimization of Multiple Energy Resources). Available online: <https://www.homerenergy.com> (accessed on 22 May 2020).
26. Government of B.C., Environmental and Climate Change. Available online: <https://www2.gov.bc.ca/gov/content/environment/climate-change/planning-and-action/carbon-tax> (accessed on 22 May 2020).
27. NASA Prediction of Worldwide Energy Resources. Available online: <https://power.larc.nasa.gov/> (accessed on 22 May 2020).
28. Hakimi, S.M.; Moghaddas-Tafreshi, S.M. Optimal sizing of a stand-alone hybrid power system via particle swarm optimization for Kahnouj area in south-east of Iran. *Renew. Energy* **2009**, *34*, 1855–1862. [CrossRef]
29. Amphlett, J.C.; Baumert, R.M.; Mann, R.F.; Peppley, B.A.; Roberge, P.R.; Harris, T.J. Performance modeling of the Ballard Mark IV solid polymer electrolyte fuel cell: I. Mechanistic model development. *J. Electrochem. Soc.* **1995**, *142*, 1. [CrossRef]
30. Canadian Weather, Climate and Hazards. Available online: <https://www.canada.ca/en/services/environment/weather.html> (accessed on 22 May 2020).
31. Pokhrel, S.; Kuyuk, A.F.; Kalantari, H.; Ghoreishi-Madiseh, S.A. Techno-Economic Trade-off between Battery Storage and Ice Thermal Energy Storage for Application in Renewable Mine Cooling System. *Appl. Sci.* **2020**, *10*, 6022. [CrossRef]
32. Energy Efficiency and Renewable Energy, Fuel Cell Technologies Office Multi-Year Research, Development, and Demonstration Plan. Available online: <https://www.energy.gov/eere/fuelcells/downloads/fuel-cell-technologies-office-multi-year-research-development-and-22> (accessed on 22 May 2020).
33. Car and Driver, Caterpillar 797. Available online: <https://www.caranddriver.com/reviews/a15140071/caterpillar-797-specialty-file> (accessed on 22 May 2020).
34. Varaschin, J.; de Souza, E. Economics of diesel fleet replacement by electric mining equipment. In Proceedings of the 15th North American Mine Ventilation Symposium 2015, Blacksburg, VA, USA, 20–25 June 2015.

35. Luta, D.N.; Raji, A.K. Optimal sizing of hybrid fuel cell-supercapacitor storage system for off-grid renewable applications. *Energy* **2019**, *166*, 530–540. [[CrossRef](#)]
36. Esposito, D.V. Membraneless electrolyzers for low-cost hydrogen production in a renewable energy future. *Joule* **2017**, *20*, 651–658. [[CrossRef](#)]
37. Fathy, A. A reliable methodology based on mine blast optimization algorithm for optimal sizing of hybrid PV-wind-FC system for remote area in Egypt. *Renew. Energy* **2016**, *95*, 367–380. [[CrossRef](#)]
38. National Laboratory of the U.S. Department of Energy. Available online: https://www.hydrogen.energy.gov/pdfs/review14/pd031_harrison_2014_o.pdf (accessed on 22 May 2020).
39. Chi, J.; Yu, H. Water electrolysis based on renewable energy for hydrogen production. *Chin. J. Catal.* **2018**, *39*, 390–394. [[CrossRef](#)]
40. Gabbar, H.A.; Abdussami, M.R.; Adham, M. Techno-Economic Evaluation of Interconnected Nuclear-Renewable Micro Hybrid Energy Systems with Combined Heat and Power. *Energies* **2020**, *13*, 1642. [[CrossRef](#)]
41. Natural Resources Canada. Retail Fuel Prices by Province-Energy Sources. 2018. Available online: <https://www.nrcan.gc.ca/energy/fuel-prices/4593> (accessed on 22 May 2020).
42. Amiri, L.; de Brito, M.A.; Baidya, D.; Kuyuk, A.F.; Ghoreishi-Madiseh, S.A.; Sasmito, A.P.; Hassani, F.P. Numerical investigation of rock-pile based waste heat storage for remote communities in cold climates. *Appl. Energy* **2019**, *252*, 113475. [[CrossRef](#)]

Publisher’s Note: MDPI stays neutral with regard to jurisdictional claims in published maps and institutional affiliations.



© 2020 by the authors. Licensee MDPI, Basel, Switzerland. This article is an open access article distributed under the terms and conditions of the Creative Commons Attribution (CC BY) license (<http://creativecommons.org/licenses/by/4.0/>).